PAPER

NCICT: a computational solution to estimate organ doses for pediatric and adult patients undergoing CT scans

IOP Publishing | Society for Radiological Protection Journal of Radiological Protection
J. Radiol. Prot. **35** (2015) 891–909 doi:10.1088/0952-4746/35/4/891

NCICT: a computational solution to estimate organ doses for pediatric and adult patients undergoing CT scans

Choonsik Lee[1,5], Kwang Pyo Kim[2], Wesley E Bolch[3], Brian E Moroz[1] and Les Folio[4]

[1] Division of Cancer Epidemiology and Genetics, National Cancer Institute, National Institute of Health, Bethesda, MD 20892, USA
[2] Department of Nuclear Engineering, Kyung Hee University, Gyeonggi-do, Korea
[3] Departments of Biomedical Engineering, University of Florida, Gainesville, FL 32611, USA
[4] Radiology and Imaging Sciences Clinical Center, National Institutes of Health, Bethesda, MD 20892, USA

E-mail: leechoonsik@mail.nih.gov

Received 17 August 2015, revised 23 September 2015
Accepted for publication 16 October 2015
Published 26 November 2015

Abstract

We developed computational methods and tools to assess organ doses for pediatric and adult patients undergoing computed tomography (CT) examinations. We used the International Commission on Radiological Protection (ICRP) reference pediatric and adult phantoms combined with the Monte Carlo simulation of a reference CT scanner to establish comprehensive organ dose coefficients (DC), organ absorbed dose per unit volumetric CT Dose Index ($CTDI_{vol}$) (mGy/mGy). We also developed methods to estimate organ doses with tube current modulation techniques and size specific dose estimates. A graphical user interface was designed to obtain user input of patient- and scan-specific parameters, and to calculate and display organ doses. A batch calculation routine was also integrated into the program to automatically calculate organ doses for a large number of patients. We entitled the computer program, National Cancer Institute dosimetry system for CT(NCICT). We compared our dose coefficients with those from CT-Expo, and evaluated the performance of our program using CT patient data. Our pediatric DCs show good agreements of organ dose estimation with those from CT-Expo except for thyroid. Our results support that the adult phantom in CT-Expo seems to represent a pediatric individual between 10 and 15 years

[5] Author to whom any correspondence should be addressed.
Investigator, Radiation Epidemiology Branch, Division of Cancer Epidemiology and Genetics, National Cancer Institute, National Institute of Health, Rockville, MD 20850, USA.

rather than an adult. The comparison of $CTDI_{vol}$ values between NCICT and dose pages from 10 selected CT scans shows good agreements less than 12% except for two cases (up to 20%). The organ dose comparison between mean and modulated mAs shows that mean mAs-based calculation significantly overestimates dose (up to 2.4-fold) to the organs in close proximity to lungs in chest and chest–abdomen–pelvis scans. Our program provides more realistic anatomy based on the ICRP reference phantoms, higher age resolution, the most up-to-date bone marrow dosimetry, and several convenient features compared to previous tools. The NCICT will be available for research purpose in the near future.

Keywords: computed tomography, organ dose, computational phantoms, Monte Carlo simulation

(Some figures may appear in colour only in the online journal)

1. Introduction

Although computed tomography (CT) provides great benefits to patients, there have been concerns about potential associated risks from radiation doses especially in pediatric patients who are more sensitive to radiation [1]. Epidemiological studies of cancer risk in patients undergoing CT require estimation of radiation dose to tissues exposed to x-ray emitted from CT scanners. Researchers have developed methods to meet the research needs as follows.

The Public Health England (PHE, formerly National Radiation Protection Board), and Helmholtz Zentrum Munchen (formerly National Research Center for Environment and Health, GSF) introduced two independent comprehensive organ dose databases. The NRPB organ dose database [2] is based on a hermaphrodite adult stylised (or mathematical) phantom and the GSF database [3, 4] is based on male and female stylised phantoms, called ADAM and EVA [5], as well as two pediatric voxel (or tomographic) phantoms [6]. Graphical user interface (GUI)-based software programs such as CTDosimetry[6] and CTDOSE [7] based on the NRPB database, and CT-Expo [8] and WinDose [9] based on the GSF database were introduced. Radimetrics™ (Bayer HealthCare LLC, Whippany, NJ), a popular computer software package for dose tracking in patients undergoing CT, x-ray, mammography, and interventional imaging, is commercially available but the organ doses are based on a series of stylised phantoms. Anatomical structures of the stylised phantoms, introduced in 1980s [10], are represented by mathematical surface equations, which are significantly limited in describing complicated human anatomy [11, 12]. It has been reported that such lack of anatomical realism in the stylised phantoms result in significant discrepancies in radiation doses when compared with the anatomy of real patients [13–15], especially in CT examinations where usually partial body is exposed to x-ray.

More recent CT dosimetry computer programs began to use voxel phantoms [11, 12, 16], which are based on medical tomographic images and represent more realistic anatomy than the previous stylised phantoms. Ban *et al* introduced a web-based CT dose calculation system, WAZA-ARI [17], which is based on a Japanese adult male voxel phantom and Particle and Heavy Ion Transport code System (PHITS). Kalender *et al* introduced ImpactDose[7], improved version

[6] www.impactscan.org/ctdosimetry.htm
[7] www.ct-imaging.de/en/ct-software-e/impactdose-e.html

of WinDose [9], by incorporating a series of stylised pediatric phantoms and the International Commission on Radiological Protection (ICRP) adult male and female voxel phantoms [18]. VirtualDose^{TM}CT (Virtual Phantoms, Inc., Albany, NY) is also the software package based on a series of pediatric and adult deformable phantoms coupled with Graphics Processing Unit (GPU)-based Monte Carlo simulation. Sahbaee *et al* [19] reported an iPhone-based software based on a mathematical model derived from the correlation between organ dose coefficients (called h factor) and the patient body size. However, the computational phantoms within some of the existing software tools are limited to patient-specific anatomies that may be different from the reference anatomy recommended by ICRP, which might be the best surrogate when CT images are not available in retrospective epidemiological studies. Although CT images are available, researchers may also use the reference phantoms if they intend to calculate organ doses for a large number of patients because it might not be feasible to extract CT images for each patient for dose calculations. Furthermore, some programs mentioned above are designed for the patient dose monitoring at large-scale clinical centres and mostly available as commercial products.

We developed computational methods to calculate several dose descriptors including organ doses for CT patients by using ICRP-adopted pediatric and adult reference voxel phantoms coupled with Monte Carlo simulation of the x-ray from CT examination. We incorporated the dose estimation methods into a graphical user interface (GUI)-based computer program for users to readily estimate organ doses for patients.

2. Materials and methods

2.1. Organ dose calculation algorithm

We developed an algorithm to calculate organ doses by combining dose coefficients (DC) that can be selected based on patient- and scan-specific parameters, and $\mathrm{CTDI_{vol}}$ obtained from the particular scan for which organ doses are calculated. The algorithm is based on the finding that $\mathrm{CTDI_{vol}}$ can be used as a normalisation factor to account for the differences among CT scanners, which was reported by Turner *et al* [20]. The algorithm is explained by the following equation:

$$D(\text{organ, age, gender,spectrum}) = \sum_{z=\mathrm{SS}}^{z=\mathrm{SE}} DC(\text{organ, age, gender, spectrum}, z) \times \mathrm{CTDI_{vol}} \quad (1)$$

where

- D (organ, age, gender, spectrum) is the absorbed dose (mGy) for the *organ* of interest, the age and gender of a given patient scanned by a scanner with a x-ray spectrum;
- SS and SE are Scan Start and Scan End, respectively, that are the distance (cm) from the top of the head in patients;
- DC(organ, age, sex, spectrum, z) is the 5D matrix of organ dose coefficient (DC) (mGy/mGy) per 1 cm axial slice: organ dose (mGy) normalised to the $\mathrm{CTDI_{vol}}$ (mGy) of the reference CT scanner used for the Monte Carlo calculations. *Organ* is the organ of interest, *age* and *sex* are from a given patient, *spectrum* is one of the six combinations of four tube potentials (80, 100, 120, and 140 kVp) and two filtrations (head and body) of a particular CT scan, and z is the slice number ranging from the top of the head to the bottom of the patient's feet;
- $\mathrm{CTDI_{vol}}$ is from the particular scan for which organ doses are calculated.

2.2. Organ dose coefficients

The algorithm described in equation (1) requires two components: DC and $CTDI_{vol}$. We calculated a comprehensive organ DC by using the ICRP reference pediatric and adult phantoms coupled with the Monte Carlo simulation of x-rays in a reference CT scanner. The ICRP published the adult male and female reference voxel phantoms [18] and more recently adopted the voxel format of the pediatric hybrid phantoms developed by the University of Florida and the National Cancer Institute [21] as their pediatric reference phantoms. To be consistent with the ICRP adult phantoms, several additional tissue models were added to the existing UF/NCI pediatric phantoms such as lymph nodes [22], muscle, and glandular tissue in breasts. The voxel resolutions range from 0.000 29 cm^3 (newborn) to 0.3653 cm^3 (adult male). The ICRP reference pediatric and adult phantoms were combined with the simulation of x-rays in a reference CT scanner (Siemens Sensation 16) within a Monte Carlo transport code, MCNPX2.7, which was previously validated [13, 14, 23]. We used a total of 10^8 particle histories in the Monte Carlo calculations to keep relative errors to smaller than 2% for the major organs included in the beam coverage.

We calculated organ doses for a total of 12 pediatric and adult male/female phantoms for consequential slice locations (from the top of the head to the bottom of the feet with 1 cm slice thickness), and for various x-ray spectra (head and body filters and 80, 100, 120, and 140 kVp) of the reference scanner. We then normalised the organ doses (mGy) to unit $CTDI_{vol}$ (mGy) of the reference scanner to derive $CTDI_{vol}$-to-organ dose coefficients (mGy/mGy). We compared the whole body scan DCs for different ICRP phantoms with those from CT-Expo based on two pediatric and two adult phantoms. For the comparison, we derived organ DCs for CT-Expo by normalising organ doses to $CTDI_{vol}$ from the head and body CTDI phantoms.

2.3. $CTDI_{vol}$ estimation

The second component in equation (1) is $CTDI_{vol}$ from a particular scan for which organ doses are calculated. Most of modern CT scanners directly provide $CTDI_{vol}$ on its dose page as well as in the Radiation Dose Structured Report (RDSR) [24]. Although the data is not directly available from some old scanners, if the scanner is available, one can measure $CTDI_{vol}$ using a CTDI phantom and ion chamber. However, if the scanner is not even available and $CTDI_{vol}$ is unknown, the value must be derived from the following equation:

$$\mathrm{CTDI_{vol}(make,\ model,\ spectrum)} = \frac{n\mathrm{CTDI_w(make,\ model,\ spectrum)}}{\mathrm{Pitch}} \times \left(\frac{I \times t}{100}\right) \times k_{\mathrm{OB}} \quad (2)$$

where

- $n\mathrm{CTDI_w}$(make, model, spectrum) is the $CTDI_w$ normalised to 100 mAs for a given scanner make and model, and x-ray spectrum, that can be selected from the CTDI library that we previously published [25] ;
- $I \times t$ (mAs) is the product of the tube current (I) and the single rotation time (t);
- k_{OB} is the overbeaming correction factor defined by Nagel *et al* [26].

2.4. Organ dose calculation for tube current modulation scans

In case of tube current modulation (TCM) scans, the equation (1) can be modified as follows, where $\mathrm{CTDI_{vol}}(z)$ is now the function of the slice location, z.

$$D(\text{organ, age, gender, spectrum}) = \sum_{z=\text{SS}}^{z=\text{SE}} [\text{DCC}(\text{organ, age, gender, spectrum}, z) \times \text{CTDI}_{\text{vol}}(z)] \,. \quad (3)$$

The slice-specific CTDI_{vol} may be directly abstracted from the Radiation Dose Structured Report (RDSR) for some modern CT scanners. If not, the values can be derived from slice-specific mAs values using equation (2), where $I \times t$ (mAs) is now the function of the slice location, z, which can be abstracted from DICOM headers.

2.5. Graphical user interface

We developed a GUI for users to conveniently input scan parameters and to calculate organ doses for CT patients by using the dose calculation algorithm explained above. The workflow in the GUI-based program is summarised in the flowchart shown in figure 1.

Other than organ doses, we also included the calculations of dose–length-product (DLP), size specific dose estimates (SSDE), and effective dose. We calculated DLP (mGy cm) from the CTDI_{vol} (mGy) and the scan length (cm) obtained from the particular scan for which organ doses are calculated. Then we used two regression equations for 16 cm and 32 cm diameter CTDI phantoms from the relationship between effective diameter (cm) and conversion factors reported by AAPM TG 204 [27]:

$$16\,\text{cm CTDI phantom} : y = 1.875\text{e}^{-0.039x} \quad (4)$$

$$32\,\text{cm CTDI phantom} : y = 3.705\text{e}^{-0.037x} \quad (5)$$

where y is the weighting factors to calculate SSDE from CTDI_{vol} and x is the effective diameter[8] (cm) measured from patients. We measured effective diameter from the 12 phantoms at each slice with the interval of 1 cm in the torso region, from which then the program will pick an appropriate effective diameter at the mid-level of the scan range. We also designed the program to calculate and display two effective doses for each phantom based on the two sets of tissue weighting factors defined by ICRP Publication 60 [28] and 103 [29]. It must be noted that the effective dose shown here for a specific male or female phantom is not consistent with its definition provided by ICRP, which is the average of male and female organ doses.

We developed the GUI-based CT dose calculator using Python computer language, which is compatible with multiple platforms including Windows, Macintosh, and LINUX operating systems. We entitled the computer program, National Cancer Institute dosimetry system for Computed Tomography (NCICT).

2.6. Batch calculation mode

In epidemiological studies for CT patients, individualised organ doses are required for generally large-scale patient cohorts. The parameters required for organ dose calculations can be collected either from old CT films or DICOM files. We designed a batch routine to import the list of parameters for a large-scale patient group and automatically export organ doses. The parameters required to calculate organ doses include: patient-related parameters (patient ID, age, gender, scan start and end locations mapped on the phantoms), scanner-related parameters

[8] Effective diameter $= \sqrt{\text{AP} \times \text{LAT}}$ where AP and LAT are the anterior posterior (AP) and lateral (LAT) dimension, respectively, of the patient's cross section on the mid-level of the scan range [27].

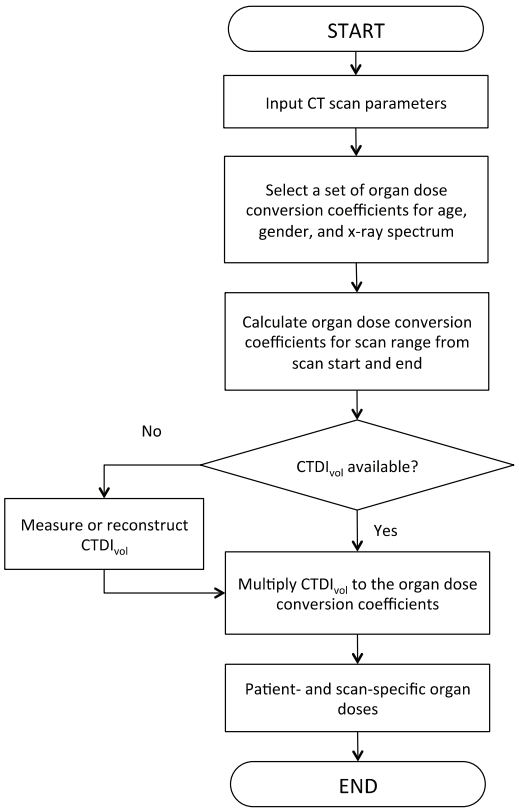

Figure 1. Flowchart of the organ dose calculation algorithm in the NCICT program.

(scanner manufacturer and model, x-ray filter, collimation width, tube potential, tube current–time product, and pitch). The parameters can be listed in an Excel spreadsheet, which can be imported into NCICT. A new Excel file will be generated containing organ doses and other dose descriptors.

2.7. Dose calculations for patients

We randomly sampled 10 patients who underwent chest, abdomen–pelvis (AP), and chest–abdomen–pelvis scans (CAP) scanned by three different scanner models (Definition DS, Biograph 128, and Flash) from Siemens (Germany) at the National Institutes of Health (NIH) Clinical Center. Slice-specific mAs values were abstracted from DICOM header using an in-house script. Average $CTDI_{vol}$ was also abstracted from the dose pages.

First, we tested if equation (2) can accurately estimate the $CTDI_{vol}$ displayed on the dose pages assuming the CT scans do not directly provide $CTDI_{vol}$, which is common in organ dose reconstructions in retrospective epidemiological studies. We derived $CTDI_{vol}$ from the scanner model, tube potential, tube current–time product, x-ray filter, and total collimation width, and compared the results with the real $CTDI_{vol}$ values displayed on the dose pages. We also compared our results with the $CTDI_{vol}$ derived from CT-Expo.

Second, we estimated organ doses for three selected patients using the closest ICRP phantoms matched for patient age, each of whom underwent chest, AP, and CAP scans using

average mAs and slice-specific modulated mAs, and compared to each other. Although the modulated tube current from DICOM headers does not accurately represent the actual angular and longitudinal changes of tube current, it is reported that the longitudinal approximated TCM function can provide organ dose estimates with the root-mean-square deviation of less than 10% [30]. Dose-length product (DLP) (mGy cm) obtained from the dose pages, the imaged scan length (cm), and $CTDI_{vol}$ (mGy) were used to derive the overrange length (cm), the half length of which was added to the start and end of the scan range using the following equation [31] :

$$DLP = CTDI_{vol} \times L_{TOT} = CTDI_{vol} \times (L_{IM} + L_{OV}) \quad (6)$$

where L_{TOT} is total exposed scan length, L_{IM} is imaged scan length, and L_{OV} is overrange length. We selected 10-, 5-, and 15 year phantoms for the 13 year (chest scan), 7 year (AP scan), and 17 year (CAP scan) patients, respectively. We created three different batch files for (1) organ dose calculations when $CTDI_{vol}$ is not available (table A1), (2) organ dose calculations when $CTDI_{vol}$ is available (table A2), and (3) organ dose calculations for TCM scans when slice-specific $CTDI_{vol}$ is available (table A3).

3. Results

3.1. Organ dose coefficients

Organ dose coefficients (mGy/mGy) for head, chest, abdomen–pelvis (AP), and chest–abdomen–pelvis (CAP) scans with the tube potential of 120 kVp from the ICRP reference pediatric and adult phantoms are tabulated in table 1. The anatomical landmarks defining the scan range were obtained from the scan protocol used in the NIH Clinical Center: the head scan ranges from the top of the head to the second cervical vertebra, the chest scan covers from the clavicles to the middle of the liver, the AP scan covers the anatomy ranging from the top of liver to the midfemoral head, and the CAP examination ranges from the clavicles to the midfemoral head. We normalised organ doses for adult head scans and pediatric head and body scans (chest, AP, and CAP) to the $CTDI_{vol}$ from the head CTDI phantom (16 cm diameter). Organ doses for adult chest, AP, and CAP scans were normalised to the $CTDI_{vol}$ from the body CTDI phantom (32 cm diameter). We removed the DCs less than 0.02 mGy/mGy from the tables.

In the head scans (table 1(a)), the brain DC for the newborn is 1.5 times greater than the value for the adult male. The DCs for all organs are equal to or smaller than the $CTDI_{vol}$ from the head CTDI phantom. Organs other than brain, pituitary gland, lens, salivary glands, oral cavity, and thyroid receive negligible doses, of which DC is less than 0.1 mGy/mGy. In the chest scan (table 1(b)), the thyroid, trachea, thymus, lungs, breast, and heart wall receive dose greater than the body $CTDI_{vol}$ in case of the adult male. Those organs in the newborn and 1 year phantoms also receive doses greater than the head $CTDI_{vol}$. The lung DC for the newborn is 1.6 times greater than the value for the 15 year male phantom. In the AP scans (table 1(c)), the stomach wall, liver, gall bladder, spleen, pancreas, kidney, small intestine, and colon received doses greater than the body $CTDI_{vol}$ in the adult male phantom, where the colon DC (1.484 mGy/mGy) is the greatest. In the CAP scans (table 1(d)), the dose trends from chest and AP scans are combined.

Figure 2(a) shows the comparison of the DCs of selected radiosensitive organs from whole body scans of the ICRP pediatric phantoms with the tube potential of 120 kVp between our calculations and CT-Expo. Our DCs show good agreements with those from CT-Expo based on the Baby (2 months) and Child (7 years) voxel phantoms except for the thyroid. The DCs of the thyroid of the Child phantom in CT-Expo are 80% and 84% of the

Table 1. Organ doses normalized to $CTDI_{vol}$ (mGy/mGy) for (a) head scans, (b) chest scans, (c) abdomen-pelvis scans, and (d) chest-abdomen-pelvis scans with the tube potential of 120 kVp. $CTDI_{vol}$ from the 16 cm CTDI phantom was used for all scans and ages except for adult body scans where $CTDI_{vol}$ from the 32 cm CTDI phantom was used.

(a) Head Scans

Normalised to	$CTDI_{vol}$ 16 cm							
Organ	00 M	01 M	05 M	10 M	15F	15 M	35F	35 M
Brain	1.049	0.906	0.830	0.809	0.781	0.752	0.767	0.717
Pituitary gland	0.941	0.796	0.777	0.748	0.725	0.660	0.605	0.690
Lens	1.092	0.962	0.962	0.896	0.961	0.943	0.863	0.850
Eye balls	1.038	1.005	0.926	0.886	0.934	0.909	0.824	0.818
Salivary glands	0.416	0.543	0.812	0.604	0.721	0.792	0.835	0.674
Oral cavity	0.391	0.837	0.919	0.819	0.612	0.719	0.733	0.565
Spinal cord	0.042	0.064	0.063	0.034	0.101	0.129	0.167	0.105
Thyroid	0.168	0.135	0.113	0.082	0.051	0.055	0.072	0.030
Esophagus	0.054	0.084	0.048	0.028	0.015	0.020	0.033	—
Trachea	0.085	0.114	0.065	0.043	0.025	0.030	0.050	0.020
Thymus	0.059	0.057	0.037	0.027	0.021	—	0.020	—
Lungs	0.039	0.035	0.034	—	—	—	—	—
Breast	0.023	—	—	—	—	—	—	—
Heart wall	0.032	0.026	—	—	—	—	—	—
Stomach wall	—	—	—	—	—	—	—	—
Liver	—	—	—	—	—	—	—	—
Gall bladder	—	—	—	—	—	—	—	—
Adrenals	—	—	—	—	—	—	—	—
Spleen	—	—	—	—	—	—	—	—
Pancreas	—	—	—	—	—	—	—	—
Kidney	—	—	—	—	—	—	—	—
Small intestine	—	—	—	—	—	—	—	—
Colon	—	—	—	—	—	—	—	—
Rectosigmoid	—	—	—	—	—	—	—	—
Bladder	—	—	—	—	—	—	—	—
Prostate	—	—	—	—	NA[a]	—	NA	—
Uterus	NA	NA	NA	NA	—	NA	—	NA
Testes	—	—	—	—	NA	—	NA	—
Ovaries	NA	NA	NA	NA	—	NA	—	NA
Skin	0.226	0.204	0.136	0.094	0.073	0.070	0.073	0.069
Muscle	0.220	0.333	0.135	0.070	0.052	0.037	0.027	0.026
Active marrow	0.305	0.357	0.299	0.159	0.095	0.111	0.050	0.048
Shallow marrow	0.486	0.294	0.269	0.168	0.129	0.138	0.141	0.129

(*Continued*)

Table 1. (*Continued*)

(b) Chest scans

Normalised to	$CTDI_{vol}$ 16 cm						$CTDI_{vol}$ 32 cm	
Organ	00 M	01 M	05 M	10 M	15F	15 M	35F	35 M
Brain	0.045	0.026	0.020	0.023	—	—	—	—
Pituitary gland	0.056	0.033	—	—	—	—	—	—
Lens	0.040	—	—	—	—	—	—	—
Eye balls	0.050	0.020	—	—	—	—	—	—
Salivary glands	0.493	0.159	0.092	0.108	0.062	0.047	0.076	0.081
Oral cavity	0.462	0.078	0.047	0.056	0.062	0.047	0.077	0.049
Spinal cord	0.712	0.551	0.412	0.242	0.296	0.211	0.563	0.523
Thyroid	1.208	1.181	1.070	0.998	0.887	0.607	0.755	1.661
Esophagus	1.047	0.875	0.779	0.642	0.616	0.561	1.043	0.969
Trachea	1.047	0.981	0.941	0.735	0.707	0.627	0.906	1.268
Thymus	1.086	1.024	0.988	0.770	0.726	0.667	1.447	1.449
Lungs	1.150	1.082	0.963	0.804	0.741	0.703	1.494	1.237
Breast	1.070	0.870	0.791	0.694	0.598	0.646	1.439	1.160
Heart wall	1.177	1.077	0.946	0.787	0.735	0.736	1.600	1.289
Stomach wall	0.870	0.550	0.414	0.272	0.339	0.297	0.669	0.699
Liver	0.979	0.663	0.491	0.413	0.445	0.393	1.007	0.762
Gall bladder	0.809	0.250	0.139	0.140	0.224	0.179	0.421	0.293
Adrenals	0.883	0.793	0.466	0.289	0.314	0.270	0.872	0.852
Spleen	1.073	0.876	0.505	0.393	0.405	0.326	1.102	0.956
Pancreas	0.678	0.175	0.128	0.121	0.118	0.101	0.218	0.251
Kidney	0.324	0.280	0.130	0.092	0.090	0.092	0.213	0.182
Small intestine	0.162	0.068	0.034	0.031	0.033	0.027	0.062	0.068
Colon	0.334	0.074	0.033	0.031	0.022	0.021	0.023	0.108
Rectosigmoid	0.066	0.022	—	—	—	—	—	—
Bladder	0.047	0.020	—	—	—	—	—	—
Prostate	0.027	—	—	—	NA	—	NA	—
Uterus	NA	NA	NA	NA	0.003	NA	0.003	—
Testes	—	—	—	—	—	—	NA	—
Ovaries	NA	NA	NA	NA	0.003	NA	0.004	NA
Skin	0.367	0.229	0.166	0.149	0.136	0.138	0.251	0.240
Muscle	0.340	0.171	0.148	0.156	0.100	0.126	0.237	0.240
Active marrow	0.428	0.345	0.197	0.192	0.179	0.173	0.375	0.314
Shallow marrow	0.464	0.391	0.310	0.226	0.174	0.152	0.372	0.264

(c) Abdomen–pelvis scans

Normalised to	$CTDI_{vol}$ 16 cm						$CTDI_{vol}$ 32 cm	
Organ	00 M	01 M	05 M	10 M	15F	15 M	35F	35 M
Brain	—	—	—	—	—	—	—	—
Pituitary gland	—	—	—	—	—	—	—	—
Lens	—	—	—	—	—	—	—	—
Eye balls	—	—	—	—	—	—	—	—
Salivary glands	0.046	0.026	—	—	—	—	—	—
Oral cavity	0.046	0.023	—	—	—	—	—	—

(*Continued*)

Table 1. (*Continued*)

Spinal cord	0.672	0.585	0.499	0.493	0.281	0.292	0.363	0.301
Thyroid	0.083	0.076	0.036	0.023	0.018	0.014	0.030	0.027
Esophagus	0.532	0.251	0.277	0.223	0.221	0.184	0.320	0.270
Trachea	0.132	0.072	0.057	0.042	0.037	0.024	0.047	0.039
Thymus	0.159	0.122	0.088	0.060	0.033	0.029	0.066	0.051
Lungs	0.652	0.494	0.260	0.218	0.194	0.182	0.395	0.309
Breast	1.009	0.816	0.754	0.442	0.323	0.376	0.150	0.333
Heart wall	0.730	0.527	0.521	0.354	0.259	0.211	0.583	0.467
Stomach wall	1.154	1.011	0.964	0.854	0.809	0.779	1.592	1.273
Liver	1.147	1.013	0.912	0.793	0.733	0.729	1.546	1.205
Gall bladder	1.099	0.998	0.961	0.834	0.711	0.716	1.406	1.229
Adrenals	1.028	0.871	0.814	0.699	0.632	0.575	1.164	0.964
Spleen	1.155	1.047	0.947	0.863	0.805	0.761	1.482	1.187
Pancreas	1.160	1.050	0.991	0.831	0.773	0.721	1.583	1.214
Kidney	1.198	1.050	1.012	0.884	0.837	0.765	1.591	1.374
Small intestine	1.165	1.053	1.069	0.958	0.844	0.811	1.510	1.439
Colon	1.201	1.088	1.114	1.010	0.932	0.914	1.619	1.484
Rectosigmoid	1.029	0.872	0.808	0.700	0.536	0.469	0.852	1.060
Bladder	1.086	0.956	0.751	0.550	0.409	0.387	1.022	1.020
Prostate	0.701	0.597	0.216	0.172	NA	0.102	NA	0.289
Uterus	NA	NA	NA	NA	0.467	NA	0.669	NA
Testes	0.157	0.190	0.139	0.085	NA	0.090	NA	0.030
Ovaries	NA	NA	NA	NA	0.537	NA	0.724	NA
Skin	0.483	0.375	0.280	0.256	0.216	0.207	0.378	0.353
Muscle	0.444	0.255	0.207	0.226	0.139	0.163	0.416	0.389
Active marrow	0.350	0.346	0.234	0.281	0.299	0.259	0.620	0.529
Shallow marrow	0.374	0.442	0.345	0.299	0.252	0.202	0.531	0.385

(d) Chest–abdomen–pelvis scans

Normalised to	$CTDI_{vol}$ 16 cm						$CTDI_{vol}$ 32 cm	
Organ	00 M	01 M	05 M	10 M	15F	15 M	35F	35 M
Brain	0.049	0.028	0.022	0.024	—	—	—	—
Pituitary gland	0.059	0.035	—	—	—	—	—	—
Lens	0.044	—	—	—	—	—	—	—
Eye balls	0.054	0.023	—	—	—	—	—	—
Salivary glands	0.501	0.167	0.097	0.111	0.063	0.048	0.078	0.083
Oral cavity	0.470	0.085	0.051	0.058	0.064	0.048	0.080	0.051
Spinal cord	0.997	0.903	0.768	0.660	0.476	0.408	0.738	0.693
Thyroid	1.223	1.202	1.080	1.006	0.891	0.611	0.762	1.669
Esophagus	1.100	0.920	0.842	0.709	0.667	0.604	1.096	1.038
Trachea	1.069	1.000	0.957	0.747	0.716	0.634	0.917	1.278
Thymus	1.110	1.054	1.012	0.788	0.734	0.674	1.461	1.463
Lungs	1.196	1.155	1.014	0.856	0.776	0.739	1.552	1.300
Breast	1.094	0.908	0.833	0.724	0.620	0.667	1.466	1.195
Heart wall	1.222	1.154	1.032	0.864	0.781	0.776	1.673	1.380
Stomach wall	1.202	1.098	1.030	0.916	0.864	0.836	1.694	1.415
Liver	1.222	1.101	0.990	0.879	0.808	0.794	1.705	1.368

(*Continued*)

Table 1. (*Continued*)

Gall bladder	1.135	1.045	0.993	0.872	0.754	0.754	1.478	1.301
Adrenals	1.080	0.980	0.886	0.765	0.683	0.626	1.220	1.032
Spleen	1.224	1.138	1.021	0.934	0.859	0.811	1.636	1.371
Pancreas	1.193	1.088	1.022	0.867	0.800	0.747	1.624	1.278
Kidney	1.227	1.100	1.045	0.913	0.859	0.787	1.634	1.422
Small intestine	1.182	1.069	1.078	0.967	0.851	0.818	1.523	1.456
Colon	1.220	1.104	1.123	1.019	0.937	0.920	1.625	1.509
Rectosigmoid	1.039	0.878	0.812	0.703	0.537	0.471	0.854	1.062
Bladder	1.092	0.961	0.754	0.551	0.410	0.388	1.023	1.021
Prostate	0.705	0.601	0.217	0.172	NA	0.103	NA	0.290
Uterus	NA	NA	NA	NA	0.468	NA	0.671	—
Testes	0.159	0.192	0.140	0.086	NA	0.090	NA	0.030
Ovaries	NA	NA	NA	NA	0.538	NA	0.725	0.000
Skin	0.644	0.501	0.382	0.359	0.306	0.301	0.550	0.530
Muscle	0.590	0.351	0.298	0.331	0.205	0.251	0.596	0.575
Active marrow	0.589	0.562	0.379	0.426	0.431	0.388	0.878	0.775
Shallow marrow	0.635	0.696	0.579	0.479	0.385	0.320	0.799	0.606

[a] NA: not available.

DCs of our 5 year and 10 year phantoms, respectively. The DCs from the CT-Expo adult phantom are compared with those from our 10-, 15 year, and adult phantoms in figure 2(b). The adult phantom of CT-Expo seems to represent a pediatric individual between 10 and 15 years rather than an adult.

3.2. A GUI-based computer program

Figure 3(a) shows the user interface for users to conveniently input CT scan parameters and calculate organ doses. Example input parameters are shown for an adult male scanned for the CAP examination using Siemens Somatom Definition Flash scanner. The interface consists of four panels: patient parameters (top left), scanner parameters (bottom left), scan range (middle), and organ dose results (right).

In the 'patient parameters' panel (top left), users can select the age and gender of a patient of interest. The height and weight of a selected phantom are displayed, which represent the ICRP reference body dimensions [32]. In the current version of NCICT, users cannot adjust the height and weight. In the 'Scan parameters' panel (bottom left), users can select the manufacturer, model, and the type of the bowtie filter of the CT scanner for which organ doses are sought. Based on the selection and the total collimation input, normalised $CTDI_w$ (mGy/100 mAs) is displayed, which is derived from the built-in CTDI library [25]. Then other scan-related parameters are entered such as pitch, tube potential (kVp), and current–time product (mAs), which will be used to calculate $CTDI_{vol}$ (mGy) and DLP (mGy cm). If a custom $CTDI_{vol}$ is available, users can directly input the number into the $CTDI_{vol}$ box and the value will override the $CTDI_{vol}$ derived from the selection of scanner models. The effective diameter (cm) at the middle level of the given scan range is selected from the previously measured data, and is used to derive SSDE (mGy) based on equation (5). In the scan range panel (middle), the front and rear views of the selected phantom are displayed with a red box representing a scan range. Users can manually adjust the scan range by dragging the upper and lower boundary of the scan range using a mouse pointer or select the

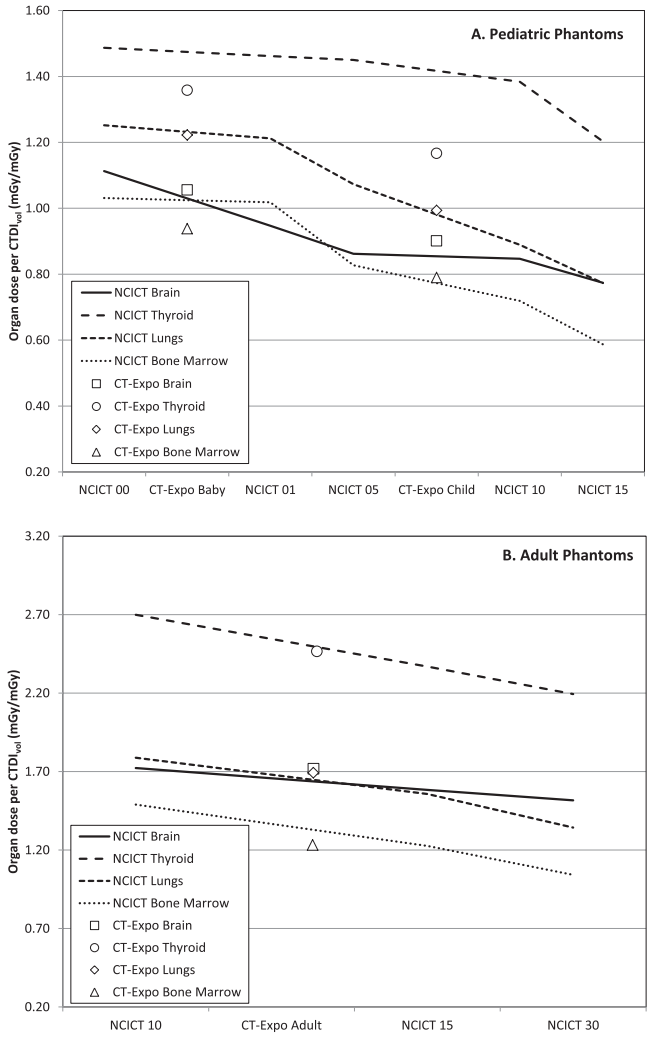

Figure 2. Comparison of dose coefficients (mGy/mGy) for (a) pediatric and (b) adult whole body scan between NCICT and CT-Expo.

predefined protocols from the list box, where the scan ranges for head, chest, AP, CAP, and head-CAP scans are included. The scan start and end locations, which is the distance from the top of the head (cm) are displayed under the predefined protocol list box. Users can also directly input the scan start and end location into the boxes and the scan range is automatically changed on the phantom view.

Whenever users adjust any parameters in the three input panels (patient parameters, scan parameters, and scan range), organ doses on the right panel are automatically calculated, and also copied to Clipboard, which can be pasted to spreadsheets or text editors. Users can simply plot the organ dose results by clicking the 'Bar Graph' button (figure 3(b)), and also copy the list of organ names to Clipboard by clicking the 'Copy organ list to Clipboard' button. NCICT has two options under 'Batch' menu: 'Batch—with $CTDI_{vol}$' and 'Batch—without $CTDI_{vol}$', which will import parameters from excel spreadsheet (tables A1 and A2).

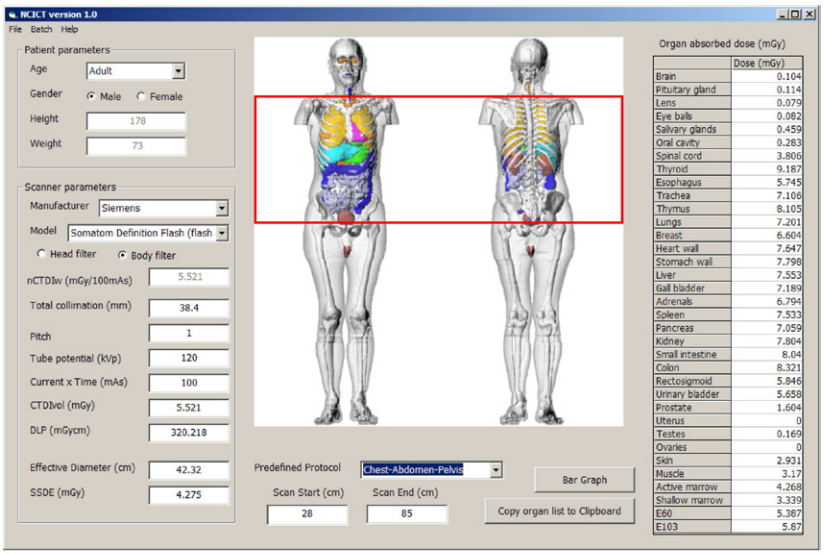

(a)

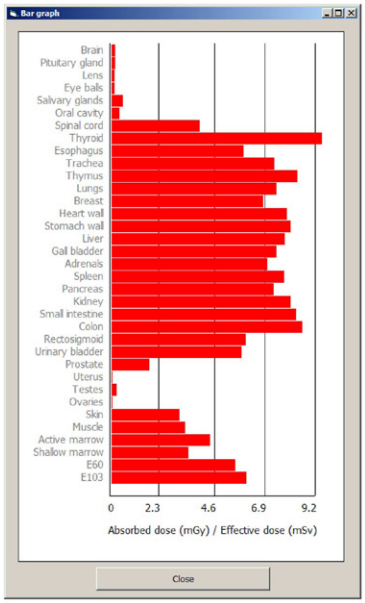

(b)

Figure 3. (a) Graphical user interface (GUI) of the NCICT program showing an example dose calculation for adult male chest–abdomen–pelvis (CAP) scan, and (b) a simple bar graph generated for the example case.

3.3. Performance evaluation

First, using the scan parameters abstracted from the 10 patients (table 2), we tested the accuracy of the $CTDI_{vol}$ derived from the scanner manufacturer and model, bowtie filter type, tube potential, current–time product, and total collimation by comparing the results

Table 2. Comparison of the $CTDI_{vol}$ derived from NCICT and CT-Expo with those abstracted from the dose pages.

Scan ID	Scanner model	Tube potential (kVp)	Total collimation (mm)	Average mAs	$CTDI_{vol}$ (mGy)				
					Dose Page	NCICT	Diff (%)[a]	CT-Expo	Diff (%)[a]
1	Definition DS	100	28.8	50	1.54	1.71	11	1.70	11
2	Definition DS	100	28.8	107	4.16	3.65	−12	3.60	−13
3	Biograph 128 PETCT	120	38.4	88	5.98	5.90	−1	5.30	−11
4	Definition Flash	100	38.4	53	2.35	2.81	20	2.00	−15
5	Definition Flash	120	38.4	83	4.60	4.60	0	4.60	0
6	Definition DS	100	28.8	63	1.96	2.17	10	2.10	7
7	Biograph 128 PETCT	120	38.4	94	6.35	6.26	−1	5.70	−10
8	Definition Flash	120	38.4	70	3.86	3.86	0	3.90	1
9	Definition Flash	100	38.4	59	2.61	3.11	19	3.10	19
10	Definition Flash	120	38.4	102	6.89	7.04	2	7.10	3

[a] Diff(%) = (NCICT or CT-Expo − Dose Page)/Dose Page × 100.

with the $CTDI_{vol}$ displayed on the dose pages. Table 2 shows the comparison of $CTDI_{vol}$ values between NCICT and dose page. Our results show good agreements less than 12% except for the two scans using Definition Flash with 100 kVp where the differences are up to 20%. We also derived $CTDI_{vol}$ values from CT-Expo, which also show agreements less than 20%.

Second, we calculated organ doses for three selected patients (chest, AP, and CAP scans) by using mean mAs and modulated mAs as shown in table 3. The results show that when we use mean mAs, dose to the organs close to the lungs will be significantly overestimated in chest and CAP scans. The breast doses from mean mAs are 1.7- (chest scan) and 2.4-fold (CAP scan) greater than those from modulated mAs. The mean mAs-based method provides 1.3- (chest scan) and 1.6-fold (CAP scan) greater heart doses compared to the modulated mAs-based method. When mean mAs is used in the AP and CAP scans, slight underestimation is observed in the bladder and prostate. Figure 4 shows the variation of $CTDI_{vol}$ derived from the modulated mAs data with the 15 year-old male phantom (bottom) used in the calculations and the sagittal view of the 17 year-old male patient (top) in the CAP scan. The pattern of the variation in $CTDI_{vol}$ is reflected to the organ doses in table 4.

4. Discussion

Compared to other existing CT dosimetry tools, our program has the following advantages. First, the organ dose coefficients are based on the ICRP reference pediatric and adult [18] phantoms, which represent the reference body size (height and weight) [32], organ mass [32], elemental composition [32, 33], and the alimentary models [34]. The up-to-date ICRP dosimetry data for active and shallow bone marrow [35, 36] was also adopted. Second, we designed a user interface for users to interactively input patient- and scanner-related parameters into the dose calculator and to obtain organ doses. The batch calculation function will be useful for dose calculations for a large-scale patient cohort, which has been utilised in multiple epidemiological studies [37–40] and studies of CT dose trends

Table 3. Comparison of organ doses from NCICT based on modulated mAs and mean mAs for chest, AP, and CAP scan patients. Organ doses were removed when those are smaller than 20% of the greatest organ dose in a given patient.

	Chest scan for 13 year Female			AP scan for 7 year Male			CAP scan for 17 year Male		
Organs	NCICT - TCM	NCICT - Mean mAs	Ratio[a]	NCICT - TCM	NCICT - Mean mAs	Ratio	NCICT - TCM	NCICT - Mean mAs	Ratio
Thyroid	2.2	2.2	0.97	—	—	—	6.9	4.7	0.68
Breasts	1.4	2.5	1.72	5.8	6.0	1.03	3.8	9.0	2.38
Esophagus	2.1	2.2	1.06	2.7	2.9	1.09	7.4	8.2	1.11
Thymus	3.1	2.7	0.87	—	—	—	14.1	9.1	0.65
Lungs	2.5	2.9	1.14	2.9	3.3	1.13	8.0	10.1	1.26
Heart	2.2	2.9	1.31	5.2	5.7	1.10	6.7	10.8	1.61
Gall bladder	0.8	1.3	1.53	7.2	7.6	1.06	9.4	10.7	1.13
Liver	1.9	2.2	1.19	7.0	7.3	1.03	8.8	11.0	1.26
Stomach	1.4	1.9	1.31	7.3	7.6	1.04	9.7	11.6	1.20
Colon	0.2	0.2	1.36	8.2	8.6	1.05	11.7	12.7	1.08
Spleen	2.1	2.6	1.22	7.2	7.5	1.03	9.7	11.1	1.15
Pancreas	0.6	0.8	1.37	7.4	7.8	1.06	9.3	10.6	1.14
Adrenals	1.5	1.9	1.22	6.2	6.4	1.03	7.5	8.6	1.15
Kidneys	—	—	—	7.5	7.9	1.06	9.7	11.0	1.13
Small intestine	—	—	—	8.1	8.4	1.03	11.2	11.7	1.04
Bladder	—	—	—	8.4	7.9	0.95	10.8	9.2	0.85
Prostate	NA[b]	NA	NA	7.6	7.3	0.96	8.4	8.2	0.98
Testicles	NA	NA	NA	6.7	7.3	1.10	8.7	9.9	1.13
Bone marrow	0.7	0.7	1.03	2.3	2.3	1.02	6.4	6.2	0.96
Bone surfaces	0.9	0.8	0.98	3.3	3.4	1.02	5.6	5.2	0.93
Skin	0.5	0.6	1.09	2.5	2.7	1.05	4.3	4.4	1.03

[a] Ratio =NCICT_Mean / NCICT_TCM.
[b] NA: Not Available.

[41, 42]. NCICT is also standalone computer software compatible with multiple platforms including Windows, Mac, and LINUX. Users do not have to rely on a central server or a web interface to compute organ doses. Third, our program provides organ dose estimates calculated using the ICRP phantoms matched for patients undergoing TCM scans. Considering the significant dose differences between the two calculation methods based on mean mAs and modulated mAs, this feature will provide more accurate organ dosimetry for patients scanned by modern CT scanners. Finally, we plan to release the NCICT program for research purpose without cost.

We note that our dose calculation program has a couple of limitations. First, the organ dose results still contain uncertainties due to a variety of sources. When $CTDI_{vol}$ is not available, the calculation must rely on the reconstruction of $CTDI_{vol}$ based on the normalised $CTDI_w$ library [25]. We tested the reconstruction algorithm only for scanners from Siemens, which must be extended to other manufacturers. Although the ICRP phantoms represent reference anatomies, the detailed anatomy of the phantoms may be different from true anatomy of patients. If patient-specific organ doses are of interest, real patient anatomy with manual organ contouring must be used. However, the approach may not be feasible for a large number of patients. Second, one cannot calculate organ doses for TCM scans if slice-specific $CTDI_{vol}$ or mAs is

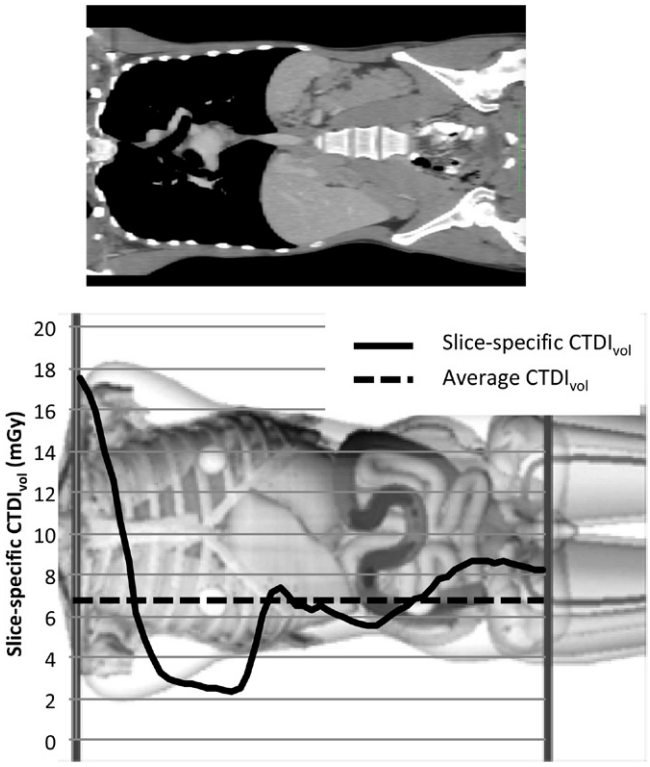

Figure 4. The pattern of the slice-specific $CTDI_{vol}$ derived from the modulated mAs with the 15 year-old phantom (top) and the sagittal view of the 17 year-old patient (bottom).

not available, which is common for retrospective CT dose calculations. However, it must be noted that it is very difficult to predict or model different kinds of TCM algorithms built in CT scanners from different manufacturers [43].

5. Conclusion

We developed computational methods to readily estimate dose descriptors including organ doses for patients undergoing CT scans, which were incorporated into a computer program, entitled NCICT. The program provides organ doses based on the ICRP reference pediatric and adult phantoms and other dose descriptors such as effective dose and SSDE through the GUI, which also include a batch calculation feature. Organ doses can be calculated for TCM scans by abstracting slice-specific mAs data from DICOM headers. NCICT will be useful for researchers to accurately estimate organ doses for pediatric and adult patients undergoing CT exams.

Acknowledgments

This work was supported by the intramural research program of the National Institutes of Health, National Cancer Institute, Division of Cancer Epidemiology and Genetics. This study utilised the high-performance computational capabilities of the Biowulf computing system at the National Institutes of Health, Bethesda, MD. (http://biowulf.nih.gov).

Appendix

Table A1. List of parameters for the batch calculation in NCICT used to calculate the column 'NCICT – Mean mAs' in table 3 *when* $CTDI_{vol}$ *is not available*. Gender ID 1 and 2 represent female and male, respectively. Filter ID 1 and 2 represent head and body bowtie filters, respectively.

ID	Scan start	Scan end	Make	Model	Age	Gender	kVp	mAs	Pitch	Filter	Collimation
4	24	46	3	13	10	1	100	53	0.6	2	38.4
8	31	63	3	13	5	2	120	70	1	2	38.4
10	28	87	3	13	15	2	120	102	0.8	2	38.4

Table A2. List of parameters for the batch calculation in NCICT used to calculate the column 'NCICT – Mean mAs' in table 3 *when* $CTDI_{vol}$ *is available*. Gender ID 1 and 2 represent female and male, respectively. Filter ID 1 and 2 represent head and body bowtie filters, respectively.

ID	Scan start	Scan end	CTDIvol	Age	Gender	kVp	Filter
4	24	46	2.35	10	1	100	2
8	31	63	3.86	5	2	120	2
10	28	87	6.89	15	2	120	2

Table A3. List of parameters for the organ dose calculation in NCICT used to calculate the column 'NCICT – Modulated mAs' in table 3 *when slice-specific* $CTDI_{vol}$ *is available*. Gender ID 1 and 2 represent female and male, respectively. Filter ID 1 and 2 represent head and body bowtie filters, respectively.

ID	Scan start	Scan end	CTDIvol	Age	Gender	kVp	Filter
4	24	24	2.59	10	1	100	2
4	25	25	2.74	10	1	100	2
4	26	26	2.71	10	1	100	2
4	27	27	2.51	10	1	100	2
4	28	28	2.36	10	1	100	2
4	29	29	2.27	10	1	100	2
4	30	30	2.19	10	1	100	2
4	31	31	1.86	10	1	100	2
4	32	32	1.70	10	1	100	2
4	33	33	1.40	10	1	100	2
4	34	34	1.22	10	1	100	2
4	35	35	0.97	10	1	100	2
4	36	36	0.85	10	1	100	2
4	37	37	0.83	10	1	100	2
4	38	38	0.92	10	1	100	2
4	39	39	1.31	10	1	100	2
4	40	40	1.67	10	1	100	2
4	41	41	1.76	10	1	100	2
4	42	42	1.81	10	1	100	2
4	43	43	1.76	10	1	100	2
4	44	44	1.76	10	1	100	2
4	45	45	1.76	10	1	100	2

References

[1] Committee to Assess Health Risks from Exposure to Low Levels of Ionizing Radiation 2006 *Health Risks from Exposure to Low Levels of Ionizing Radiation* (Washington, DC: National Academies Press)

[2] Jones D G and Shrimpton P C 1991 *Survey of CT Practice in the UK. Part 3: normalised organ doses calculated using Monte Carlo techniques* (Didcot: National Radiologic Protection Board)

[3] Zankl M, Panzer W and Drexler G 1991 *The Calculation of Dose from External Photon Exposures Using Reference Human Phantoms and Monte Carlo Methods, Part VI: Organ Doses From Computed Tomographic Examinations* (Munchen: GSF-Gesellschaft fur Strahlen und Umweltforschung mbH)

[4] Zankl M, Panzer W and Drexler G 1993 *Tomographic Anthropomorphic Models. Part II: Organ Doses from Computed Tomographic Examinations in Paediatric Radiology* (Munchen: GSF-Gesellschaft fur Strahlen und Umweltforschung mbH)

[5] Kramer R, Zankl M, Williams G and Drexler G 1982 *The Calculation of Dose from External Photon Exposures Using Reference Human Phantoms and Monte-Carlo Methods, Part 1: The Male (ADAM) and Female (EVA) Adult Mathematical Phantoms* (Neuherberg: GSF-National Research Center for Health and Environment)

[6] Veit R, Zankl M, Petoussi N, Mannweiler E, Williams G and Drexler G 1989 *Tomographic Anthropomorphic Models, Part I: Construction Technique and Description of Models of an 8 Week-Old Baby and a 7 Year-Old Child* (Neuherberg: GSF-National Research Center for Environment and Health)

[7] Le Heron J C 1993 *CTDOSE: A User's Guide* (Christchurch, New Zealand)

[8] Stamm G and Nagel H D 2002 CT-expo—a novel program for dose evaluation in CT *RöFo: Fortschr. Geb. Röntgenstrahlen Nuklearmedizin* **174** 1570

[9] Kalender W A, Schmidt B and Zankl M 1999 A PC program for estimating organ dose and effective dose values in computed tomography *Eur. Radiol.* **9** 555–62

[10] Cristy M and Eckerman K F 1987 *Specific Absorbed Fractions of Energy at Various Ages from Internal Photon Sources* (Oak Ridge, TN: Oak Ridge National Laboratory)

[11] Zaidi H and Xu X G 2007 Computational anthropomorphic models of the human anatomy: the path to realistic Monte Carlo modeling in radiological sciences *Annu. Rev. Biomed. Eng.* **9** 471–500

[12] Xu X G 2014 An exponential growth of computational phantom research in radiation protection, imaging, and radiotherapy: a review of the fifty-year history *Phys. Med. Biol.* **59** R233–302

[13] Lee C, Kim K P, Long D, Fisher R, Tien C, Simon S L, Bouville A and Bolch W E 2011 Organ doses for reference adult male and female undergoing computed tomography estimated by Monte Carlo simulations *Med. Phys.* **38** 1196–206

[14] Lee C, Kim K P, Long D and Bolch W E 2012 Organ doses for reference pediatric and adolescent patients undergoing computed tomography estimated by Monte Carlo simulation *Med. Phys.* **39** 2129–46

[15] Liu H, Gu J, Caracappa P F and Xu X G 2010 Comparison of two types of adult phantoms in terms of organ doses from diagnostic CT procedures *Phys. Med. Biol.* **55** 1441–51

[16] Caon M 2004 Voxel-based computational models of real human anatomy: a review *Radiat. Environ. Biophys.* **42** 229–35

[17] Ban N, Takahashi F, Sato K, Endo A, Ono K, Hasegawa T, Yoshitake T, Katsunuma Y and Kai M 2011 Development of a web-based CT dose calculator: WAZA-ARI *Radiat. Prot. Dosim.* **147** 333–7

[18] ICRP 2009 Adult Reference Computational Phantoms *ICRP Publication 110, Ann. ICRP* **39** 1–166

[19] Sahbaee P, Segars W P and Samei E 2014 Patient-based estimation of organ dose for a population of 58 adult patients across 13 protocol categories *Med. Phys.* **41** 072104

[20] Turner A C, Zankl M, DeMarco J J, Cagnon C H, Zhang D, Angel E, Cody D D, Stevens D M, McCollough C H and McNitt-Gray M F 2010 The feasibility of a scanner-independent technique to estimate organ dose from MDCT scans: using $CTDI_{vol}$ to account for differences between scanners *Med. Phys.* **37** 1816

[21] Lee C *et al* 2010 The UF family of reference hybrid phantoms for computational radiation dosimetry *Phys. Med. Biol.* **55** 339–63

[22] Lee C, Lamart S and Moroz B E 2013 Computational lymphatic node models in pediatric and adult hybrid phantoms for radiation dosimetry *Phys. Med. Biol.* **58** N59–82

[23] Long D J, Lee C, Tien C, Fisher R, Hoerner M R, Hintenlang D and Bolch W E 2013 Monte Carlo simulations of adult and pediatric computed tomography exams: validation studies of organ doses with physical phantoms *Med. Phys.* **40** 13901
[24] Sechopoulos I, Trianni A and Peck D 2015 The DICOM radiation dose structured report: what it is and what it is not *J. Am. Coll. Radiol.: JACR* **12** 712–3
[25] Lee E, Lamart S, Little M P and Lee C 2014 Database of normalised computed tomography dose index for retrospective CT dosimetry *J. Radiol. Protect.* **34** 363–88
[26] Reiser M F, Takahashi M, Modic M and Becker C R 2004 *Multislice CT* ed M F Reiser *et al* (Berlin: Springer)
[27] AAPM 2011 *Size-Specific Dose Estimates (SSDE) in Pediatric and Adult Body CT Examinations*
[28] ICRP I 1991 ICRP Publication 60: 1990 Recommendations of the International Commission on Radiological Protection *ICRP Publication 60, Ann. ICRP*
[29] ICRP 2007 The 2007 Recommendations of the International Commission on Radiological Protection *ICRP Publication 103, Ann. ICRP* **37** 1–332
[30] Khatonabadi M, Zhang D, Mathieu K, Kim H J, Lu P, Cody D, Demarco J J, Cagnon C H and McNitt-Gray M F 2012 A comparison of methods to estimate organ doses in CT when utilizing approximations to the tube current modulation function *Med. Phys.* **39** 5212–28
[31] W H 2010 Overranging at multi- section CT: an underestimated source of excess radiation exposure 1 *Radiographics* **30** 1057–67
[32] ICRP 2002 Basic anatomical and physiological data for use in radiological protection: reference values *ICRP publication 89, Ann. ICRP* **32** 1–277
[33] ICRU 1992 *Photon, Electron, Proton and Neutron Interaction Data for Body Tissues* vol 46 (Bethesda, MD: International Commission on Radiation Units and Measurements)
[34] ICRP 2006 Human alimentary tract model for radiological protection *ICRP publication 100, Ann. ICRP* **36** 1–336
[35] Hough M, Johnson P, Rajon D, Jokisch D, Lee C and Bolch W 2011 An image-based skeletal dosimetry model for the ICRP reference adult male: internal electron sources *Phys. Med. Biol.* **56** 2309
[36] Johnson P B, Bahadori A A, Eckerman K F, Lee C and Bolch W E 2011 Response functions for computing absorbed dose to skeletal tissues from photon irradiation—an update *Phys. Med. Biol.* **56** 2347
[37] Pearce M S *et al* 2012 CT scans in childhood and risk of leukaemia and brain tumours: authors' reply *Lancet* **380** 1736–7
[38] Thierry-Chef I *et al* 2013 Assessing organ doses from paediatric CT scans: a novel approach for an epidemiology study (the EPI-CT study) *Int. J. Environ. Res. Public Health* **10** 717–28
[39] Meulepas J M *et al* 2014 Leukemia and brain tumors among children after radiation exposure from CT scans: design and methodological opportunities of the Dutch Pediatric CT Study *Eur. J. Epidemiol.* **29** 293–301
[40] Journy N, Rehel J-L, Ducou Le Pointe H, Lee C, Brisse H, Chateil J-F, Caer-Lorho S, Laurier D and Bernier M-O 2015 Are the studies on cancer risk from CT scans biased by indication? Elements of answer from a large-scale cohort study in France *Brit. J. Cancer* **112** 185–93
[41] Smith-Bindman R *et al* 2012 Use of diagnostic imaging studies and associated radiation exposure for patients enrolled in large integrated health care systems, 1996–2010 *J. Am. Med. Assoc.* **307** 2400–9
[42] Miglioretti D L, Zhang Y, Johnson E, Lee C L, Morin R L, Vanneman N V and Smith-Bindman R S-B 2014 Personalized technologist dose audit feedback for reducing patient radiation exposure from CT *J. Am. Coll. Radiol.* **11** 300–8
[43] Khatonabadi M, Kim H J, Lu P, McMillan K L, Cagnon C H, DeMarco J J and McNitt-Gray M F 2013 The feasibility of a regional $CTDI_{vol}$ to estimate organ dose from tube current modulated CT exams *Med. Phys.* **40** 051903–12